Reliability Analysis of Low-Silver BGA Spheres Comparing Failure Detection Criteria

by
Briana Fredericks

A senior project submitted in partial fulfillment of the requirement for the degree of Bachelor of Science in Industrial Engineering

California Polytechnic University
San Luis Obispo

Graded by:_____ Date of Submission:_____
Checked by:_____ Approved by:_____

Abstract

One of the challenges of solder joint reliability tests is estimating the time of failure of the solder joint. Failure criteria should be able to detect solder joint failure as early as possible, while minimizing the probability of false detection. The failure mechanism under study is cracks due to thermal fatigue. The most common method to estimate failure due to cracks is to monitor the resistance during testing, because solder imaging and cross-sectioning methods are destructive. Current industry failure criteria do not adequately demonstrate the relationship between the size of the crack and the resulting change in resistance. This project analyzes data from a thermal fatigue reliability study of low-silver ball grid array spheres. Traditional quality control charts are used to estimate the time-to-failure of the solder joints, as well as observe common failure trends. These time-to-failure estimates are compared to the IPC standard of 20% increase from initial resistance. Three common failure trends are discussed, and the reliability parameters are estimated. The results show that there is no statistically significant difference between the time-to failure estimates of the IPC standard and traditional control chart method.

Table of Contents

List of Figures

List of Tables

Chapter 1: Introduction

When a consumer purchases an electronic item, there is an expectation that the item will perform its intended function for a certain amount of time. Since solder provides the mechanical and electrical continuity in electronic assemblies, it is imperative that the solder is reliable for the product to be functional. In order to produce reliable electronics, manufacturers use Design for Reliability techniques as well as conduct reliability tests for solder to ensure that their product will not fail throughout its intended operating life. Economic factors largely affecting electronics reliability include the trend toward electronics miniaturization and the Restrictions on Hazardous Substances (RoHS) directive in 2006, which banned the use of lead and other substances in electronics. As a result of the directive, the cost of engineering change has been enormous for electronics manufacturers, and an ample understanding of the reliability of electronics using different solder composition has been difficult to achieve.

To solve this problem, a considerable amount of research has been conducted to study the reliability of lead-free solder alternatives. The goal of these reliability studies is to estimate the lifetime of the product under study and understand the modes of failure. One of the challenges in reliability testing of solder is determining the point at which the solder has failed. Solder failure occurs when the solder joint cracks, resulting in a large increase in resistance. Resistance is carefully monitored during the tests to detect these failures. However, the relationship between the crack area and the resulting change in resistance has not been established by existing failure criteria. In order to gain more meaningful results from reliability studies, further investigation of failure criteria is required.

This project analyzes data from a thermal fatigue reliability study using traditional control charts as defined by Pan and Silk [10], and compares the results to the IPC standard of 20% rise in resistance using a paired t-test. Common failure trends are discussed, and reliability parameters are estimated.

Chapter 2: Background

Reliability is an essential aspect to well engineered products. Consumers experience reliability as a problem when their television, car, computer, or cell phone suddenly is not functioning. Product failures in the airline and military industries could put people's lives at risk. In the manufacturing industry, too many failures within the warranty period would be costly. Reliability is an engineering uncertainty; we do not know exactly when a product will fail. However, probability and statistics can be applied to predict this. Reliability is defined as "the probability that an item will perform a required function without failure under stated conditions for a stated period of time." [1]

Reliability can begin as early as the product development stage. Design problems should be detected as early as possible to avoid extremely high costs of design change further in the course of the product design cycle. The idea of designing reliability into the product as early as the product development stage is called Design for Reliability (DFR). The process flow can be seen in Figure 1.

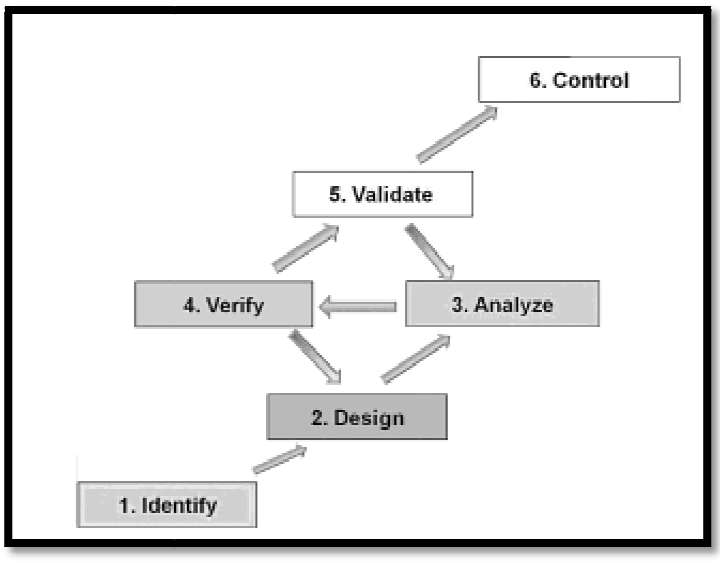

Figure 1: Design for Reliability Flow [1]

During the Identify stage, it is important to understand the customer, product environment and reliability requirements. Quality Function Deployment (QFD) is a common tool to use at this stage. During the Design stage, the reliability engineer

should work to understand the product design and possible modes of failure. A useful tool during this stage is Failure Modes, Effects and Criticality Analysis (FMECA). Additionally, supplier reliability should be addressed. During the Analyze phase, models should be developed to understand the physics of failures. Finite Element Analysis (FEA) is a valuable tool for calculating stresses that can be used in physical models. At the Verify stage, a hardware prototype should be available for testing. Common tests at this stage are Accelerated Life Tests (ALT), Highly Accelerated Life Tests (HALT), degradation analysis or reliability growth modeling. These tests identify failure mechanisms, evaluate design robustness and study the reliability of the product over time. The Validate stage is meant to ensure that the product design and process are fully functional, and any issues in these areas have been resolved. The goal of the Control phase is to maintain process control by minimizing variation. For example, Environmental Stress Screening (ESS) can be applied to units before they are shipped to the customer; products are tested beyond specification limits to stimulate any latent defects due to production or design weakness [1].

Reliability has a strong presence in the electronics industry and is often difficult to achieve due to the complexity of the devices and manufacturing processes. Solder is vital to the reliability of electronics because it provides the electrical and mechanical continuity required for a device to function. Solder reliability has been especially difficult to achieve due to the Restrictions on Hazardous Substances (RoHS) directive in 2006, which banned the use of lead (as well as other substances) in electronics [2]. The electronics industry had been using tin-lead (SnPb) solder for decades, and their entire manufacturing processes have been designed around the thermal and mechanical properties of SnPb solder. The costs associated with this change have been enormous. In 2005, Intels's director of sustainable development, Timothy Mohin, stated "The cost to get from lead to no-lead solders is substantial and thus far we have spent upwards of $100 million [3]." In addition to the large costs of design and process change, an understanding of the reliability of electronics using different solder composition has been difficult to achieve.

The most common replacement for SnPb solder has been varying compositions of the tin-silver-copper (SnAgCu) alloy. One difference between SnPb and SnAgCu is the higher melting temperature of SnAgCu, which requires a higher peak reflow temperature during the reflow process. Also, decreased wetting ability and increase in voids observed in SnAgCu joints make the solder joints potentially less reliable than SnPb [4]. It is imperative that the reliability of these new solder alloys is well understood, so that electronic devices may be well-designed and properly manufactured.

Chapter 3: Literature Review

Failure Modes and Mechanisms

There are three basic failure modes for electronic packages: electronic shorts, opens, or intermittent failures. Each of these failures can be caused by design problems, material characteristics, or manufacturing process defects [5].
There are several material characteristics that can influence the reliability of solder joints. Table 1 shows a summary of these characteristics and their impact on reliability.

Table 1: Printed Circuit Board Materials and Reliability [5]

Material Characteristics	Impact on Reliability
Coefficient of thermal expansion	Solder joint fatigue life
Moisture absorption	Metal migration, corrosion, delamination
Glass transition temperature	Coefficient of thermal expansion (CTE) via solder joint life
Dielectric constant	High speed electrical performance
Thermal stability	CTE, reflow process, solder joints, package seal integrity
Dimensional stability	Shorts between conducting elements, laminate warp and bow
Voltage breakdown	High-pot test
Laminate adhesion	Metallization integrity
Dissipation factor	
Flammability	Fire susceptibility
Surface and volume resistivity	Surface insulation resistance

Failures due to material characteristics of low silver Ball Grid Array (BGA) packages will be the focus of this project. The SAC alloy family – a combination of tin, silver and copper – has been a common replacement for SnPb (tin lead) solder. It is common to have 3-4% silver composition in this alloy; however, suppliers have been reducing the percent composition in their sphere alloys. Some benefits of this decision include reduction in material cost, improvement of drop shock performance, reduced tin oxidation, improved wetting ability, and reduced surface roughness. However, it does raise some reliability concerns. Lower silver content

BGA spheres have a higher melting point, which is problematic during the reflow process, particularly the peak reflow temperature range [14]. If the BGA solder spheres and component paste do not fully fuse together, it will likely affect the reliability of the solder joints.

Accelerated Life Testing

As mentioned in the background, there are several methods that can test the reliability of solder joints. Testing long-term degradation at normal operating conditions is time consuming and impractical, so Accelerated Life Testing (ALT) is used to assess the solder joint degradation in a reasonable amount of time. ALT's subject test assemblies to higher than normal stresses that can be mechanical, chemical, thermal, or electrical. The applied stress induces specific failure modes and mechanisms that would occur during normal operating conditions. For example, an electronic component could be subjected to accelerated vibration tests to assess failure modes such as solder joint cracks, wire bond fracture, and fatigue fracture. The overall goal of ALT's is to conduct tests, gather failure data and estimate the lifetime distributions of the components at normal stress levels [5].

Accelerated Thermal Cycling

Accelerated Thermal Cycling (ATC) is an ALT used to assess the failure mode of creep, fatigue, and microstructural changes in solder joints [6]. Coefficient of Thermal Expansion between solder and the material to which it is bonded, thermal stability, and moisture absorption are some of the material characteristics that can affect the lifetime of solder joints under testing (as well as normal operating conditions). The act of turning a computer on, using it for a certain period of time, then turning it off is an example of a normal use that ATC is simulating over a shorter period of time. In order to accelerate the normal use condition, appropriate maximum/minimum temperature limits, dwell times, and ramp rates must be established. IPC 9701 is an industry standard for developing representative temperature cycling profiles (Figure 2).

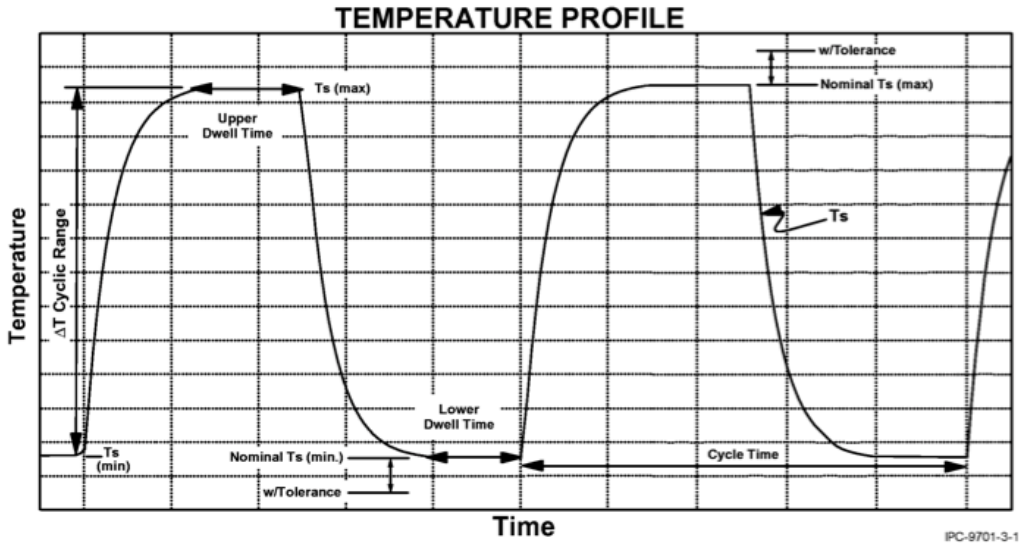

Figure 2: Theoretical Temperature Cycling Profile [7]

The minimum and maximum temperatures must be beyond the product specification limits to accelerate the test; however, the minimum and maximum temperatures must not exceed the product design limits. For example, choosing a maximum temperature outside the glass transition temperature would most likely result in unrepresentative failures. Additionally, dwell times should be chosen such that they are long enough to complete the creep process relative to normal product use [8]. The effect of ramp rate on the ATC process is not well understood. However, studies have shown that ramp rate can be load dependent and must be verified for the load being tested [9].

Failure Detection Methods

One of the challenges often faced during ATC is determining when the solder joint fails. The eventual failure of solder during ATC is a result of a crack [6]. There are two main types of cracks that result in a solder joint failure. The first is the crack initiation stage, which is detected at the first sign of a crack. The second is the crack propagation stage, which continues from the detectable crack to a full open, resulting in electrical discontinuity [10]. Images of crack initiation and propagation can be seen below in Figure 3.

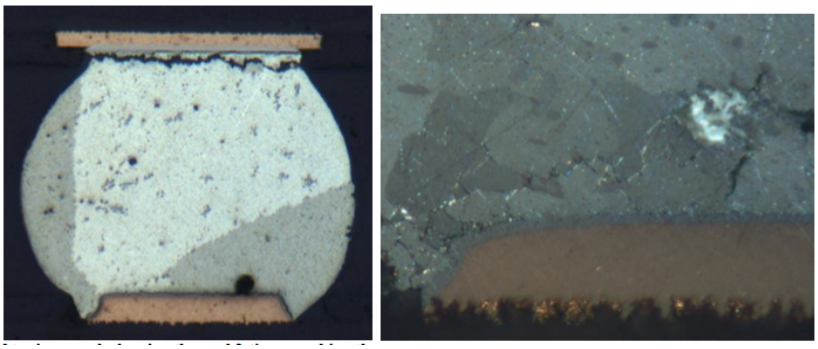

Figure 3: Full solder crack (left) and crack initiation (right) [10]

How would one determine when a crack is present? X-ray images can be used, but they are often not useful because the resolution is too low to capture the small size of the crack. Other methods, such as cross-sectioning, scanning electron microscopy (SEM), and dye-and-pry are destructive and cannot be used for continuous monitoring. Due to these difficulties, researchers rely on continuous resistance monitoring techniques to detect electrical discontinuity due to cracks [10]. Institute for Interconnecting and Packaging Electronic Circuits (now IPC Association Connecting Electronics Industries) and JEDEC (Solid State Technology Association) are the two industry standards used for monitoring failures during reliability tests. Table 2 compares some of the common standards for monitoring resistance during temperature cycling, drop tests, and bend tests.

Table 2: Summary of Failure Criteria Standards [10]

Standard	Test	Failure definition	
		Event Detector	**Data Logger**
IPC-SM-785 (1992)	**Temperature cycling**	The 1st event of resistance exceeding 1000 Ω for lasting >1 μs, followed by >9 events within 10% of the number of cycles to initial failure	
IPC-9701 (2002) & IPC-9701A (2006)	**Temperature cycling**	The 1st event of resistance exceeding 1000 Ω for lasting >1 μs, followed by >9 events within 10% of the cycles to initial failure	20% resistance increase in 5 consecutive readings
JESD22-B111 (2003)	**Drop test**	The 1st event of resistance > 1000 Ω for a period of >1μs, followed by 3 additional such events during 5 subsequent drops.	1st detection of resistance value of 100 Ω if initial resistance is <85 Ω, or 20% increase in resistance if initial resistance is >85 Ω, followed by 3 additional such events during 5 subsequent drops.
IPC/JEDEC-9702 (2004)	**Bend test**	20% resistance increase. A lower or higher threshold may be more appropriate, depending upon test equipment capability and specific daisy-chain design scheme.	

IPC-SM-785 has been the industry standard for temperature cycling since 1992. It was revised in 2002 and replaced by IPC-9701A in 2006. IPC-9701A updated the previous standards to include a failure definition when using a data logger system in addition to an event detector [10].

A study was conducted by Henshall, et al. [11] to determine the thermal fatigue resistance of low-silver BGA alloys using ATC. Three failure criteria were used to construct the Weibull curves used in reliability analysis. The first failure criterion used data logger software that detected a failed solder channel using the IPC-9701A standard criterion of a 20% resistance rise. Since resistance (R) is a function of temperature (T), R(T) was measured throughout the ATC tests and compared to the resistance of the first temperature cycle, $R_o(T)$. A failure was recorded if the following condition was true: $R(T) > 1.2R_o(T)$. It is notable that this criteria

measures resistance against more than one single reference temperature. The second criterion used was a 500 Ω resistance measurement; initial resistance was 2.5Ω to 5Ω. The third and final criterion was the detection of infinite resistance, which represents a hard open. The study concluded that the IPC-9701A standard provided the most sensitive measure of failure, detecting failures 200-500 cycles sooner than the 500 Ω and infinite resistance criterion. The 500 Ω and infinite resistance criterion gave very similar Weibull parameters, but with slightly lower slope than the IPC criteria. It was concluded that the IPC-9701A standard was the highest performing criterion for product qualification. However, it was suggested that the 500 Ω and infinite resistance criterion could be useful for a materials study due to less scattered experimental results.

A study conducted by Pan and Silk [10] uses traditional control charts ($\overline{X}$ and R) to monitor the natural, random variation of resistance of solder joints under drop and vibration reliability tests. A failure is defined as resistance exceeding a threshold that is *k* times the range of natural variation in resistance measurements. This method does not depend on the initial resistance value of solder joints. It is based on natural variation in resistance caused by variables such as measurement system and test setup.

The theory behind X-bar and R charts is defined in Montgomery's Quality Control [12]. To gather the appropriate data, the resistance of each daisy chain subgroup is collected *n* times. These measurements are averaged and become the subgroup average $\overline{X}$. Additionally, the range (R) of each subgroup is computed. The control limits for the construction of $\overline{X}$ and R charts is shown below in Table 3.

Table 3: Equations for the Traditional Control Chart Limits

	$\bar{\bar{X}}$ Chart	R chart	$\bar{\bar{X}}$ is the average of subgroup averages $\bar{R}$ is the average of subgroup ranges k is the number of standard deviations from the center n is the rational subgroup size d_2, D_3, and D_4 are constants
Upper Control Limit	$\bar{\bar{X}} + \frac{K\bar{R}}{d_2\sqrt{n}}$	$D_4\bar{R}$	
Center	$\bar{\bar{X}}$	$\bar{R}$	
Lower Control Limit	$\bar{\bar{X}} - \frac{k\bar{R}}{d_2\sqrt{n}}$	$D_3\bar{R}$	

The typical k value used for process control in industry is k =3 (for 3σ limits). In this study Pan and Silk recommend using k =10 so that failures can be detected as early as possible while still minimizing the possibility of false failure detection (Type II Error). This study has demonstrated that it is possible to detect full solder cracks using traditional control charts. This method, along with existing failure detection methods, is unable to detect partial cracks in solder due to the fact that partially cracked solder joints still have electrical continuity.

Chapter 4: Experimental Design

The data analyzed in this project was generated from a series of low-silver BGA experiments conducted by Henshall, et al. [14]. The series of experiments focused on reflow requirements, thermal reliability, and mechanical reliability of low silver BGA spheres. This project focuses on the data gathered from the thermal fatigue reliability studies.

The experimental setup involves six sphere alloys and two paste alloys. The six sphere alloys are:

- SACX 0307 – Sn-0.3Ag-0.7Cu+ Bi+X
- SAC 105 – Sn-1.0Ag-0.5Cu
- LF35 – Sn-1.2Ag-0.5Cu + 0.05Ni
- SAC 205 – Sn-2.0Ag-0.5Cu
- SAC 305 – Sn-3.0Ag-0.5Cu (Pb-free baseline)

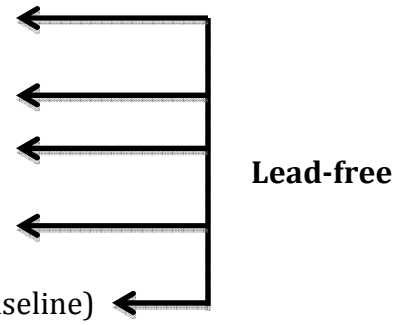

- Sn-Pb – Sn-37Pb (Eutectic Sn-Pb baseline)

The two paste alloys are:

- SAC 305
- Sn-Pb – Sn-37Pb

These solder spheres and pastes were differentiated into two types of test assemblies as follows:

Mixed Joints

- Components balled with Pb-free spheres and assembled with Sn-Pb paste

Unmixed Joints

- Components balled with Pb-free spheres and assembled with SAC305 paste (100% Pb-free)

- Components balled with eutectic Sn-Pb spheres and assembled with eutectic Sn-Pb paste (100% Sn-Pb)

Four ball grid array (BGA) package types were included in the study and can be seen in Table 4.

Table 4: BGA Package Types

BGA	Pitch (mm)	Inputs/Outputs	Solder Ball Volume (mm^3)
SuperBGA	1.27	600	0.230
Plastic BGA	1.0	324	0.131
ChipArray BGA	0.8	288	0.051
ChipArray Thin Core BGA	0.5	132	0.014

The test vehicle PCB (Figure 4) has three of each type of BGA package. During the manufacturing of the test assemblies, peak reflow temperature was either 215°C, 220°C, or 235°C. More details about the test vehicle and assembly can be seen in the reports ([15], [16]).

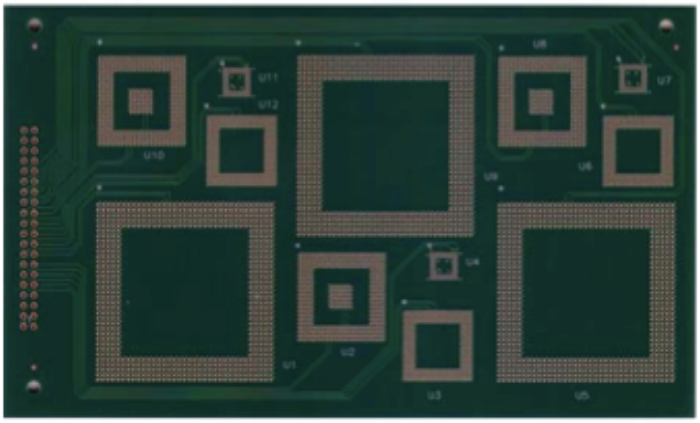

Figure 4: Test Vehicle PCB [14]

Two accelerated thermal cycling profiles were used in this study from IPC 9701A. The first profile target conditions were from 0°C to 100°C with 10 minute ramps, 10

minute dwells, and a total cycle time of 40 minutes. The second profile target conditions were from -40°C to 120°C with 16.5 minute ramps, 10 minute dwells, and a total cycle time of 53 minutes.

One daisy-chain (channel) was measured for each BGA package. The resistance was monitored for each daisy-chain using a continuous data collection system. The 0°C to 100°C test was terminated after 10,068 cycles and the -40°C to 125 °C test was terminated after 3,556 cycles. An experimental matrix for this test setup can be seen in Table 5. A total of 20 packages were tested for each treatment cell, and empty cells show that no packages were tested for that treatment.

Table 5: Complete Experimental Matrix for Accelerated Thermal Cycling Tests

Paste Alloy	Sphere Alloy	Peak Reflow T(°C)	No. of Channels Tested at 0°C to 100°C				No. of Channels Tested at -40°C to 125 °C			
			BGA Pitch (mm)				BGA Pitch (mm)			
			0.5	0.8	1.0	1.27	0.5	0.8	1.0	1.27
Sn-Pb	Sn-Pb	215	20	20	20	20	20	20	20	20
Sn-Pb	SAC105	215	20	20	20	20	20	20	**20**	20
Sn-Pb	SAC105	220			20	20			20	20
Sn-Pb	SAC205	215								
Sn-Pb	SAC305	215	**20**	20	20	20	20	20	20	20
Sn-Pb	SACx	215	20	20	20	20	20	20	20	20
Sn-Pb	LF35	215	20				20			
SAC305	SAC105	235	20	20	20	20	20	20	**20**	20
SAC305	SAC205	235	20	20	20	20	20	20	20	20
SAC305	SAC305	235	**20**	20	20	20	20	20	20	20
SAC305	SACx	235	20	20	20	20	20	20	20	20
SAC305	LF35	235	20				20			

Chapter 5: Analysis

The analysis is divided into three sections: (1) Data Preparation, (2) Control Chart Analysis, and (3) Reliability Analysis. The following treatments were analyzed:

- 0°C to 100°C Thermal Profile – 40 channels
    - SAC 305 sphere, SnPb paste, 0.5 mm pitch, 215°C reflow
    - SAC 305 sphere, SAC 305 paste, 0.5 mm pitch, 235°C reflow
- -40°C to 125°C Thermal Profile – 40 channels
    - SAC 105 sphere, SnPb paste, 1.0 mm pitch, 215°C reflow
    - SAC 105 sphere, SAC 305 paste, 1.0 mm pitch, 235°C reflow

The goal of the traditional control chart is to find the failure time for each solder channel. Once time to failure data are found, the method effectiveness will be studied to see whether traditional control charts or the IPC standard of 20% rise in resistance identified channel failure earlier. The third section, Reliability Analysis, will use the time-to-failure data to understand the failure and characteristic life of the channels.

Data Preparation

The manipulation of the given data was a lengthy process. The data was provided in individual workbooks, which contained the resistance, cycle time and other details needed for each channel (Figure 5). A total of over 1,400 workbooks were provided, with roughly 43,000 rows of data in each workbook. This data needed to be consolidated and formatted properly for efficient analysis in JMP software.

Time Elapsed	Temperature	Cycle Count	Failure	Resistance	Date/Time
600	63.24608994	0	0	4.125	10/26/2009 12:45:42 PM
1201	101.7978973	0	0	4.339844	10/26/2009 12:55:42 PM
1802	72.69140625	0	0	4.175781	10/26/2009 1:05:43 PM
2405	1.249022961	0.5	0	3.746094	10/26/2009 1:15:46 PM
3007	17.20800972	0.5	0	3.847656	10/26/2009 1:25:48 PM
3609	95.51074219	1	0	4.310547	10/26/2009 1:35:50 PM
4211	102.2080002	1	0	4.361328	10/26/2009 1:45:52 PM
4813	18.98340034	1	0	3.869141	10/26/2009 1:55:54 PM
5414	-0.80078131	1.5	0	3.736328	10/26/2009 2:05:55 PM
6017	62.38378906	1.5	0	4.134766	10/26/2009 2:15:58 PM

Figure 5: Excerpt of Original Data Provided for Channel 14

First, a treatment (set of 20 channels) was decided upon for analysis. A worksheet explaining the assembly matrix and wiring chart was used to determine which solder channels were included in the decided treatment. A macro was used to combine the 20 individual workbooks into one workbook containing 20 spreadsheets, each spreadsheet corresponding to an individual solder channel.

Next, some features of each spreadsheet were manually changed. A column was added to convert the given cycle counts from decimals to whole numbers using the round function. This was necessary for the determination of subgroups and JMP analysis, as described in more detail in the following section. Also, the column names for cycles and resistance were changed so that they could be easily analyzed and labeled in JMP. An example of these manual changed can be seen in red in Figure 6.

Time Elapsed	Temperature	Cycle Count	Failure	Channel 2593 Cycles	Channel 2593 Resistance (ohms)	Date/Time
600	63.2460899	0	0	1	2.935547	10/26/2009 12:45:42 PM
1201	101.797897	0	0	1	3.058594	10/26/2009 12:55:42 PM
1802	72.6914063	0	0	1	2.976563	10/26/2009 1:05:43 PM
2405	1.24902296	0.5	0	1	2.689453	10/26/2009 1:15:46 PM
3007	17.2080097	0.5	0	1	2.761719	10/26/2009 1:25:48 PM
3609	95.5107422	1	0	2	3.058594	10/26/2009 1:35:50 PM
4211	102.208	1	0	2	3.080078	10/26/2009 1:45:52 PM
4813	18.9834003	1	0	2	2.771484	10/26/2009 1:55:54 PM
5414	-0.80078131	1.5	0	2	2.689453	10/26/2009 2:05:55 PM
6017	62.3837891	1.5	0	2	2.945313	10/26/2009 2:15:58 PM

Figure 6: Excerpt of Manipulated and Formatted Data for Channel 14

The final step for JMP analysis preparation was consolidating the cycles and resistance columns for each channel into a single worksheet so that it may be easily copied and pasted into JMP. This was done using a macro, which copied the two red columns above from all 20 worksheets (channels) in the workbook and pasted them into a single, consolidated worksheet. The data preparation process described in this section required just over an hour to complete.

Control Chart Analysis

The first step in control chart analysis is to determine rational subgroup sizing. For this particular study, it is important that a subgroup falls within one temperature cycle. Figure 7 shows the resistance versus time trend, which follows the same trend of the temperature cycling profile. The main criteria when determining subgroups within a cycle was that at least one data point was taken near each peak temperature per cycle, and the spread of samples was even throughout the cycle. It is notable that the data does not have equal sample sizes for each cycle. Throughout the experiment, sample sizes range from 4 to 6, which is the suggested sample size for establishing traditional control charts [12]. If the sample size becomes too large, the possibility of falsely detecting a failure increases because the control limits become narrower.

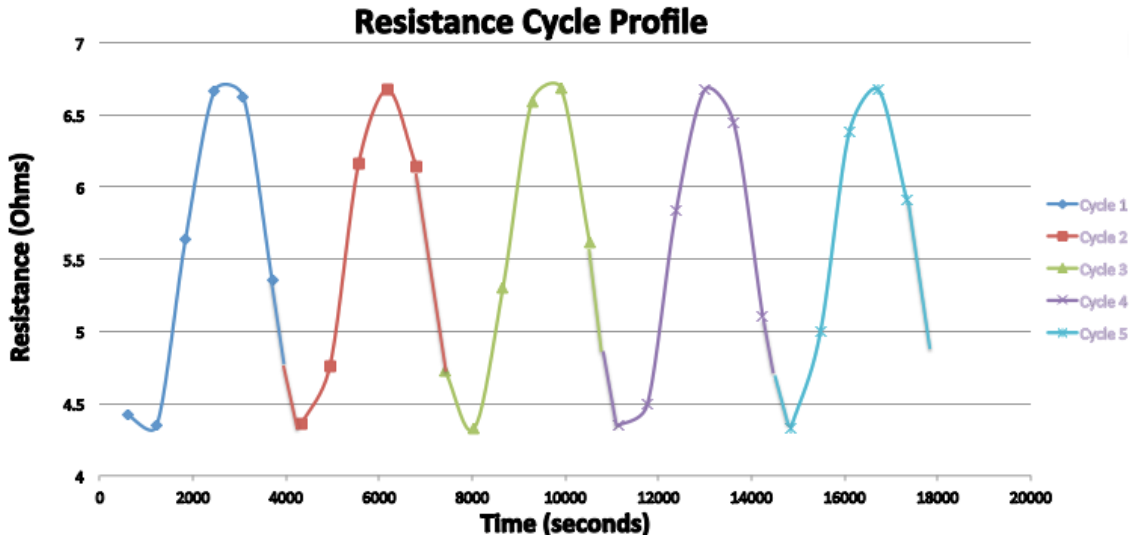

Figure 7: Resistance Profile Showing Subgroups as Cycles

Another decision to make when creating traditional control charts is the value of *k*. The typical *k* value used in industry is *k*=3, but the *k* value varies depending on application. The study discussed in the literature review by Pan and Silk [10] suggests a *k* value between 3 and 10, with a higher value reducing the possibility of false failure detection (Type I error). For this analysis, a *k* value of 5 is used.

Due to the lengthy test time required for reliability analysis, there are thousands of subgroups (temperature cycles) to be analyzed. Trial control charts using the first 40 cycles were used to generate the control limits, because this will best represent the initial resistance values that are desirable to reference as thermal cycling progresses. An example of trial control charts is shown in Figure 8.

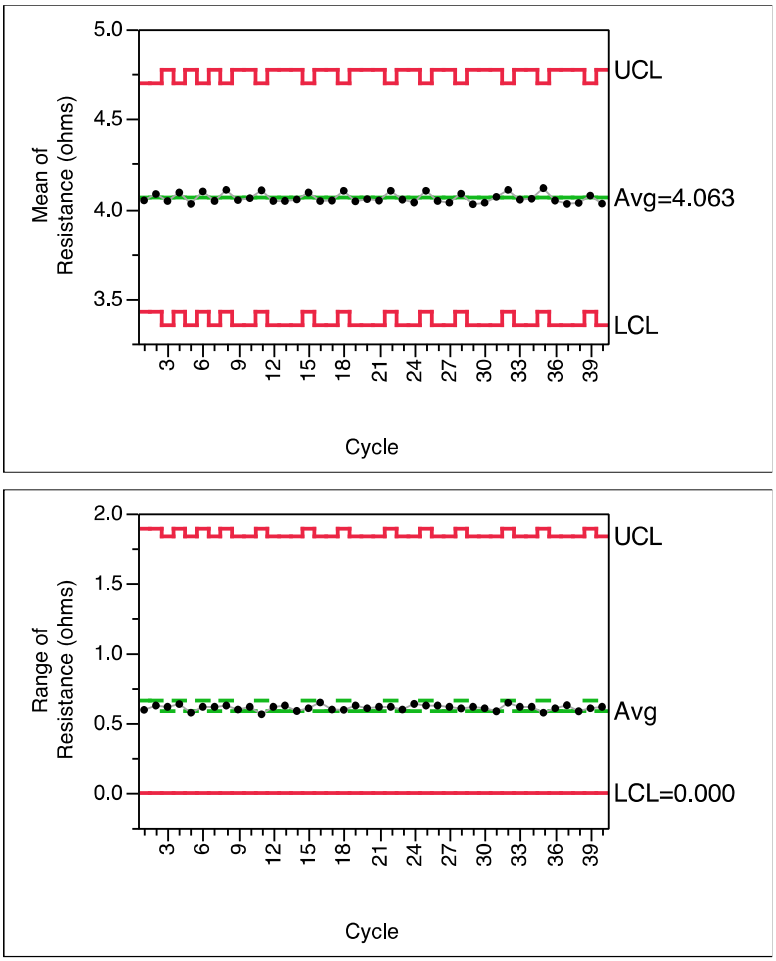

Figure 8: Control Charts for Channel 14 (SAC 305 Ball, SnPb Paste, 0.5 Pitch)

Trial charts were made for each channel and checked for any out of control conditions. For Figure 8, the Upper Control Limit (UCL) of the $\bar{X}$ chart is estimated at 4.75, and the UCL of the R Chart is estimated as 1.85. Similarly, the control limits for each channel were estimated, saved, and applied to future charts for analyzing the remaining cycles.

The next step in analyzing the control charts is the determination of a failure for the solder channel. Continuing with Channel 14, control charts for cycles 41 through 3,010 were generated. In cycle 3,011 resistance becomes infinite, making the chart difficult to scale and read for the rest of the test (total testing time is 10, 068 cycles).

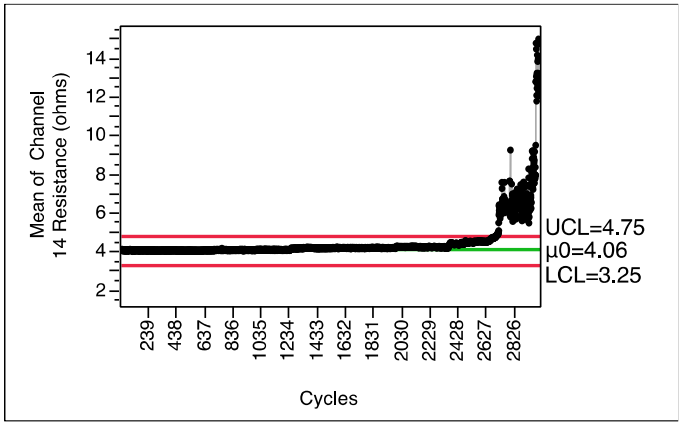

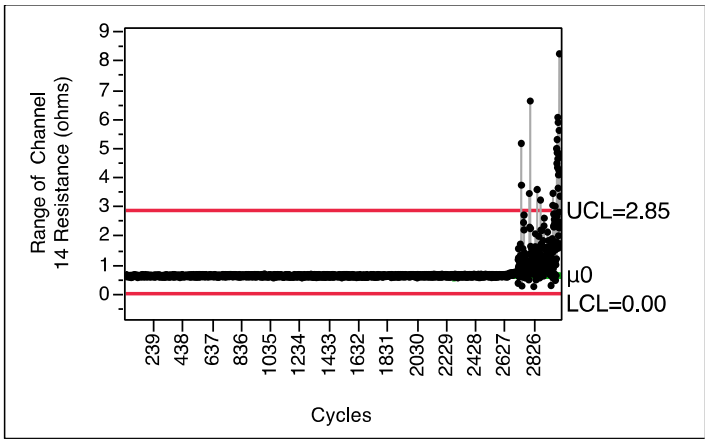

Figure 9 : Control Charts for Cycles 41 – 3,010 of Channel 14

As seen in Figure 9 these charts are clouded with data points and difficult to read. However, it is clear that Channel 14 fails sometime after 2,627 cycles. But when exactly does this channel fail?

One answer to this question could be that the channel fails at the first instance that it is out of control on the $\bar{X}$ Chart. Figure 10 takes a closer look at the trend before failure occurs. Around 2,660 cycles, the average resistance per cycle begins so slowly increase from 4.5 Ohms and approach the UCL.

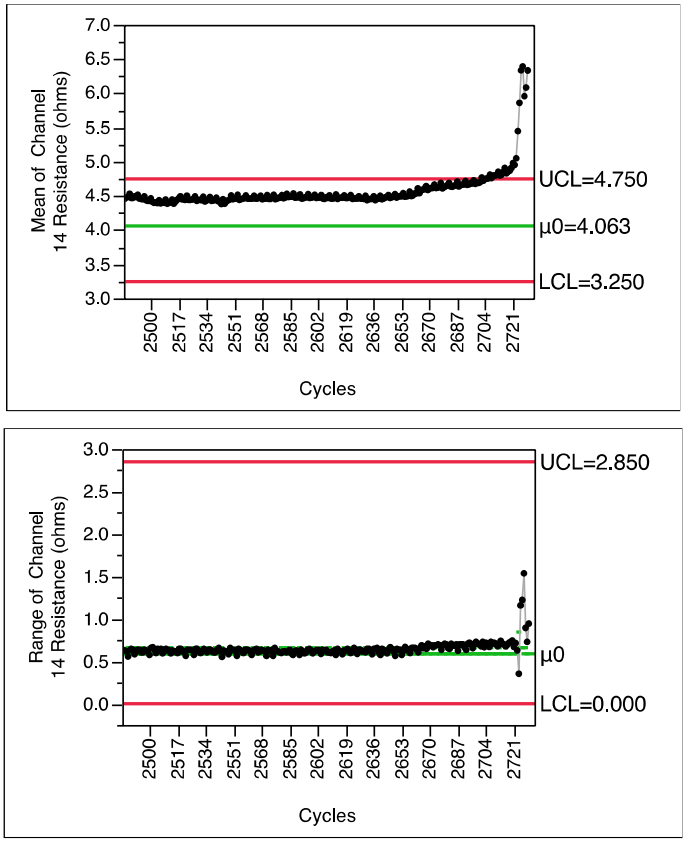

Figure 10: Control Charts for Cycles 2,484 to 2,730 of Channel 14

For Channel 14, the first occurrence that the resistance exceeds the UCL is 2,702 cycles. This is shown more clearly in Figure 11 with the blue arrow.

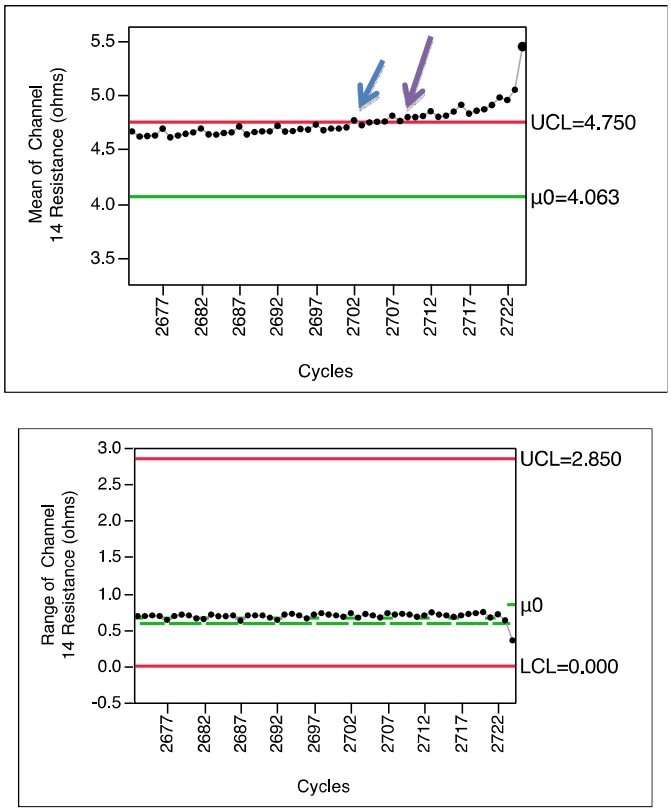

Figure 11: Control Charts Showing Point of Failure of Channel 14

One problem with this method of determining failure is that the resistance will occasionally hover around the UCL before continuing to increase. For this reason, this project will define the point of failure as the first instance resistance exceeds the UCL and continues to stay above the UCL. For Channel 14, the point of failure is 2,707 cycles (purple arrow).

Reliability Analysis

The final part of the data analysis is the reliability analysis. Once the selected treatments were prepared and analyzed using the above methods, time-to-failure data for each treatment (Appendix) was fit to a reliability distribution in JMP. The best-fit distribution is the distribution with the smallest AIC value. From the initial JMP analysis, the Lognormal and Weibull distribution had small AIC values. Since the Weibull distribution was used for analysis in the report by Henshall, et al. [14], the parameter estimates were determined using the Weibull distribution.

Chapter 6: Results and Discussion

Before presenting the results of differences in failure detection criteria, some common trends observed in the charts will be discussed. While analyzing the data using traditional control charts, some common trends that were observed were: (1) a sudden jump in resistance indicating an obvious point of failure, (2) a steady, linear increase in resistance, and (3) quick, swinging jumps between infinite resistance and just above the upper control limit.

An example of the first trend, a sudden jump in resistance indicating an obvious point of failure, can be seen in Figure 12.

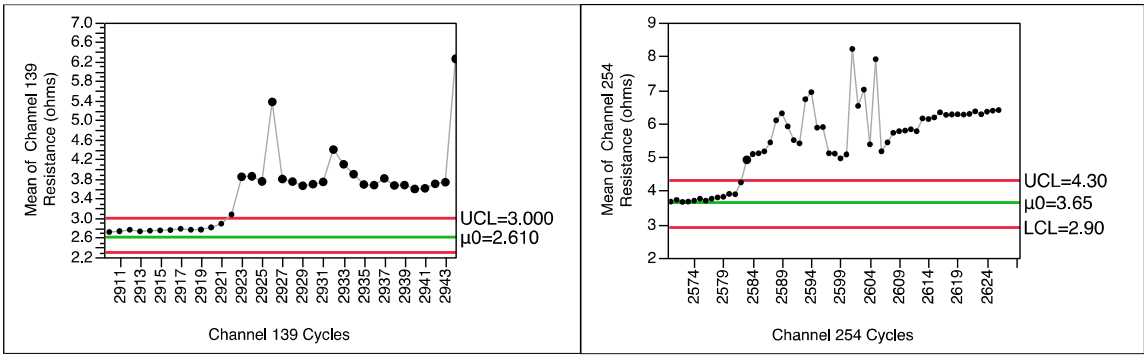

Figure 12: Trend of Sudden Increase in Resistance for Channel 139 (left) and 254 (right)

This trend occurred 78% of the time in the 0°C to 100°C profile and 43% of the time in the -40°C to 125°C profile. The data points begin hovering just above the process mean, and within about 5 cycles jump above the upper control limit. The size of the jump observed for this trend was roughly 1-2 Ohms. For these cases, the traditional control charts and the 20% increase in resistance criteria identified time-to-failure within 1 cycle. For example, traditional control charts found Channel 139 failed at 2,922 cycles, and the 20% increase criteria found Channel 139 failed at 2,923 cycles.

The second trend, a steady linear increase in resistance, can be seen in Figure 13.

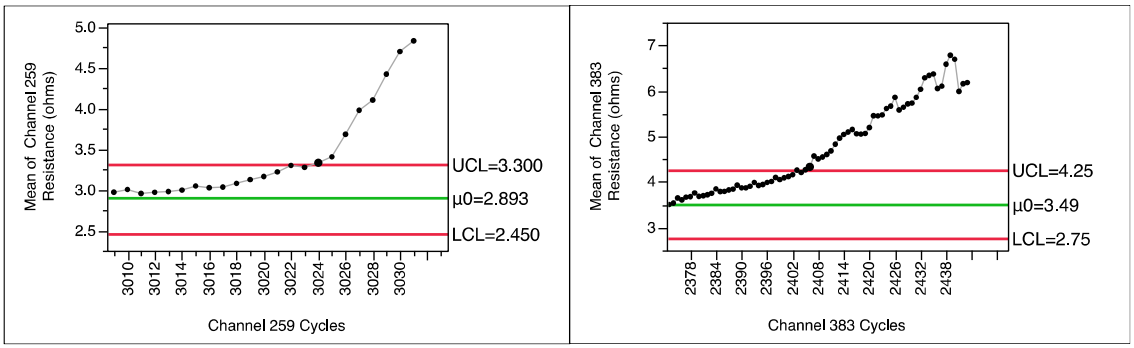

Figure 13: Trend of Continuous Increase in Resistance for Channel 259 and 383

This trend occurred 18% of the time in the 0°C to 100°C profile and 3% of the time in the -40°C to 125°C profile. It is characterized by steady, small increases in resistance for longer periods of time. For instance, Channel 383 shows an increase of less than 2 Ohms over 50 cycles. In contrast, Channel 254 in Figure 12 has the same change in resistance in about 10 cycles. For these cases, traditional control charts identified failures over 5 cycles sooner than the 20% increase criteria. It is also notable that for this case, the time-to failure using traditional control charts is highly dependent on the value of *k* chosen in the development of the charts. Recall that k= 5 was used for these charts; a smaller *k* would have detected the failure sooner, and a larger *k* value would detect failure in later cycles.

The third trend, swinging jumps between "infinite" resistance and just above the upper control limit, can be seen in Figure 14.

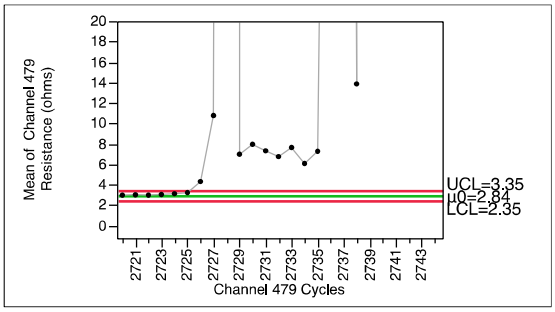

Figure 14: Trend of Flickering Resistance for Channel 479

This trend occurred 5% of the time in the 0°C to 100°C profile and 55% of the time in the -40°C to 125°C profile. For this case, the resistance increased above the upper control limit, indicating a possible failure. The interesting behavior occurred after

the failure, as Channel 479 shows. Resistance would increase "infinitely" (well over 500 Ohms) and come back down to a resistance just above the upper control limit. In these cases, it appears a crack has occurred but may be making an on and off connection, like a flickering light. Both failure criteria identified failure at 2,726 cycles. This case does not have a large impact on failure criteria definition.

Once all of the charts were analyzed, a paired t-test was used to compare the time-to-failure estimates of traditional control charts and the IPC Standard 20% increase in resistance criteria. The paired t-test was used because it blocked any variation between individual channels. At the 95% confidence level, it cannot be concluded that there is a difference between the IPC standard and Control Chart method (

Table 6). This can be observed by the very close mean-time-to-failure estimates for each treatment, and it can be statistically verified with the p-value of 0.310.

Table 6: Paired t-test Results Comparing Failure Criteria

Treatment		Mean Time-to-Failure Estimate (Cycles)		P-Value
		Control Chart	IPC Standard	
0°C to 100°C	SAC305 Ball, SnPb Paste, 0.5 mm pitch	3,499.3	3,499.6	0.310
	SAC305 Ball, SAC305 Paste, 0.5 mm pitch	2,671.1	2,672.2	
-40°C to 125°C	SAC105 Ball, SnPb Paste, 1.0mm pitch	1,736.85	1,736.6	
	SAC105 Ball, SAC305 Paste, 1.0mm pitch	1,587.65	1,587.35	

Although the paired t-test results show that there is no statistically significant difference between the two failure detection methods, a reliability analysis was conducted to check the effect of failure criteria on the reliability parameter estimates. These results are shown below in Table 7.

Table 7: Reliability Estimates Comparing Failure Criteria

Treatment		Estimates	IPC Standard	Control Charts
0°C to 100°C	SnPbBall, SAC305 Paste, 0.5mm pitch	Weibull α	3,183.49	3,182.36
		Weibull β	2.894	2.892
	SAC305 Ball, SAC305 Paste, 0.5mm pitch	Weibull α	3,675.74	3,675.39
		Weibull β	9.407	9.404
-40°C to 125°C	SAC105 Ball, SnPb Paste, 1.0mm pitch	Weibull α	1,841.67	1,841.44
		Weibull β	8.067	8.065
	SAC105 Ball, SAC305 Paste, 1.0mm pitch	Weibull α	1,677.37	1,677.07
		Weibull β	9.435	9.431

As with the paired t-test results, the Weibull parameter estimates show very little difference between the IPC standard and traditional control chart time-to-failure estimates.

Chapter 7: A Social, Economic, and Environmental Perspective

As mentioned in the background, the need for the study analyzed in this project stems from the European Union's Restriction of Hazardous Substances (RoHS) Initiative to remove lead from the manufacturing of electronics. This initiative became effective in the United States in 2006, and requires manufacturers to use less than 0.1% lead in electronic components. This initiative improves both the social and environmental aspects of electronics manufacturing. Occupational health is improved because workers in solder manufacturing plants are not exposed to the high volume of lead, which is toxic when inhaled or ingested. Public health is also improved. The Waste Electrical and Electronic Equipment (WEEE) Directive in the EU and UK encourages the design and production of electrical and electronic equipment to facilitate its repair, re-use, disassembly and recycling at end-of-life.[18] Although it is not yet required in the US, US companies must comply with the regulations when selling to companies in the EU. Both RoHS and WEEE have a substantial push on electronics manufacturers to improve social and environmental consequences of electronics designs. The results of this project add knowledge and understanding to the behavior and reliability estimates of these newer, more socially and environmentally friendly lead-free solders.

The economic aspect of compliance with WEEE and RoHS has raised much concern. Consider the market impact resulting from a shift in demand from solder metals. In the U.S., Electronics is a $400 billion-per-year industry facing significant legislative and market pressures to phase out the use of lead-based solder and switch to lead-free alternatives. A study conducted by the US Environmental Protection Agency [17] conservatively estimated that 44 million pounds of tin-lead solder was consumed in the United States in 2002, and over 176 million pounds were consumed worldwide. The lead market would drastically decrease and a subsequent increase in Tin, Silver, Copper and/or Bismoth would occur, depending on which lead-free solder alternative is most commonly used. The EPA study concluded that the decrease in demand for lead as a result of any of the conversions would be over

$5.9 million. In addition to the market effects, individual companies have suffered substantial capital costs, operating costs, and R&D costs. Examples of capital costs associated with RoHS compliance include retooling of equipment used for lead-based manufacturing and purchase of any new equipment. Operating costs increase due to increase in electricity required for manufacturing lead-free alternatives, higher costs for lead-free alternative materials (e.g. silver), and lower process efficiency. Additional losses include obsolete inventory and increase in administrative paperwork to demonstrate compliance. Increased R&D costs have been incurred to develop, test and re-qualify products, components and sub-assemblies using lead-free substances. The results of this project will lead to a better understanding of solder joint R&D, specifically for solder joint failures resulting from cracks.

Chapter 8: Conclusion

It can be concluded from this project that traditional control charts and the IPC standard of 20% rise in resistance do not provide statistically different time-to-failure estimates. Although the paired t-test and reliability parameters showed that traditional control chart estimates do not significantly differ from the IPC standard, the use of traditional control charts more clearly demonstrate the shift in mean resistance due to natural variation. These charts can be very useful for narrowing down the industry standards by further analyzing the trends shown in this report. For future studies, it is recommended to standardize the data collection method for control chart analysis, so that it may be more easily analyzed. Additionally, CUSUM charts could be used along with traditional ($\overline{X}$ and R) control charts to narrow the failure criteria definition, as they have the potential to detect smaller shifts in the mean. The final recommendation for future analysis would be to use solder imaging or cross sectioning to verify the crack size at the time-to-failure estimate.

References

[1] O'Connor, Patrick, and Andre Kleyner. *Practical Reliability Engineering*. Chicester: John Wiley and Sons, 2012.

[2] Kostic, Andrew D., Ph. D. "Lead Free Electronics Reliability." *Nasa.gov*. The Aerospace Corporation, Aug. 2011. Web. 9 Nov. 2012. <http://nepp.nasa.gov/whisker/reference/tech_papers/2011-kostic-pb-free.pdf>.

[3] Lemon, Sumner. "Cost of Intel's Lead-free Move Hits $100M, and Counting." *InfoWorld*. The IDG Network, 16 Mar. 2005. Web. 09 Nov. 2012. <http://www.infoworld.com/t/hardware/cost-intels-lead-free-move-hits-100m-and-counting-181>.

[4] J. Wang, D.M. Shaddock, and J. Pan, "Lead-free Solder Joint Reliability – State of the Art and Perspectives" Proceedings of the 37th International Symposium on Microelectronics: Long Beach, CA (2004).

[5] Viswanadham, Puligandla, and Pratap Singh. *Failure Modes and Mechanisms in Electronic Packages*. New York: Chapman & Hall, 1998, pp. 71-73.

[6] Lau, John H. *Solder Joint Reliability: Theory and Applications*. New York: Van Nostrand Reinhold, 1991.

[7] IPC-9701, "Performance Test Methods and Qualification Requirements for Surface Mount Solder Attachments," Association Connecting Electronics Industries, 2002.

[8] T. Mattila, H. Xu, O. Ratia, M. Paulasto-Krockel, "Effects of thermal cycling parameters on lifetimes and failure mechanism of solder interconnections," Proceedings of 60th Electronic Components and Technology Conference (ECTC), June 2010, pp.581-590.

[9] Y.S. Chan, S.W.R. Lee, "Detailed investigation on the creep damage accumulation of lead-free solder joints under accelerated temperature cycling," 11th International Conference on Thermal, Mechanical & Multi-Physics Simulation, and Experiments in Microelectronics and Microsystems (EuroSimE), April 2010, pp.1-6, 26-28.

[10] J. Pan and J. Silk, "A Study of Solder Joint Failure Criteria," Proceedings of 44th International Symposium on Microelectronics, Long Beach, CA, 2011, pp. 694-702.

[11] G. Henshall, J. Bath, S. Sethuraman, D. Geiger, A. Syed, M.J. Lee, K. Newman, L. Hu, D. H. Kim, W. Xie, W. Eagar and J. Waldvogel, "Comparison of Thermal Fatigue Performance of SAC105 (Sn-1.0Ag-0.5Cu), Sn- 3.5Ag, and SAC305 (Sn-3.0Ag-0.5Cu) BGA Components with SAC305 Solder Paste," Proceedings of IPC APEX 2009.

[12] Montgomery, Douglas C. *Introduction to Statistical Quality Control*. New York: Wiley, 1985.

[13] Hawkins, Douglas M., and David H. Olwell. *Cumulative Sum Charts and Charting for Quality Improvement*. New York: Springer, 1998. Print.

[14] G. Henshall, C. Shea, R. Pandher, A. Syed, Q. Chu, N. Tokotch, L. Escuro, M. Lapitan, G. Ta, A. Babasa, G. Wable, "Low-Silver BGA Assembly, Phase I – Reflow Considerations and Joint Homogeneity Reliability Assessment Initial Report," Proceedings of APEX, Las Vegas, NV, 2008.

[15] G. Henshall, M. Fehrenbach, C. Shea, Q. Chu, G. Wable, R. Pandher, K. Hubbard, G. Ramakrishna, A. Syed, "Low-Silver BGA Assembly, Phase II – Reliability Assessment. Sixth Report: Thermal Cycling Results for Unmixed Joints," SMTA International Conference Proceedings, 2010.

[16] G. Henshall, M. Fehrenbach, C. Shea, Q. Chu, G. Wable, R. Pandher, K. Hubbard, G. Ramakrishna, A. Syed, "Low-Silver BGA Assembly, Phase II – Reliability Assessment. Seventh Report: Mixed Metallurgy Solder Joint Thermal Cycling Results," Proceedings of IPC APEX, 2011.

[17] United States. Environmental Protection Agency. Office of Pollution Prevention and Toxics. *Solders in Electronics: A Life-Cycle Assessment Summary*. EPA-744-S-05-001. 2005. < http://www.epa.gov/opptintr/ dfe/pubs/solder/lca/lca-summ2.pdf>.

[18] European Commission. *Study on RoHS and WEEE Directives*. By DG Enterprise and Industry. 6-11925-AL. 2008. < http://www.rsjtechnical.com/ images/ Documents/RoHSreview_simplification_Mar08.pdf>.

Appendix

Cycles to Failure Estimates for Traditional Control Charts and IPC Standard

Channel	Paste	Ball	BGA Pitch	Reflow Temp	Board	TTF Control	TTF 20%
268	SnPb	SAC105	1.0 mm	215	3_10	1711	1711
270	SnPb	SAC105	1.0 mm	215	3_10	1827	1827
274	SnPb	SAC105	1.0 mm	215	3_10	1513	1512
388	SnPb	SAC105	1.0 mm	215	3_11	1897	1897
390	SnPb	SAC105	1.0 mm	215	3_11	1645	1645
394	SnPb	SAC105	1.0 mm	215	3_11	1507	1507
484	SnPb	SAC105	1.0 mm	215	3_12	1813	1812
486	SnPb	SAC105	1.0 mm	215	3_12	1626	1626
490	SnPb	SAC105	1.0 mm	215	3_12	1615	1615
580	SnPb	SAC105	1.0 mm	215	3_13	2139	2139
582	SnPb	SAC105	1.0 mm	215	3_13	2181	2181
586	SnPb	SAC105	1.0 mm	215	3_13	1886	1886
666	SnPb	SAC105	1.0 mm	215	3_14	1018	1018
670	SnPb	SAC105	1.0 mm	215	3_14	1784	1784
28	SnPb	SAC105	1.0 mm	215	3_8	1506	1505
30	SnPb	SAC105	1.0 mm	215	3_8	1609	1609
34	SnPb	SAC105	1.0 mm	215	3_8	1785	1784
148	SnPb	SAC105	1.0 mm	215	3_9	1988	1987
150	SnPb	SAC105	1.0 mm	215	3_9	1998	1998
154	SnPb	SAC105	1.0 mm	215	3_9	1689	1689
316	SAC305	SAC105	1.0 mm	235	8_10	1868	1868
318	SAC305	SAC105	1.0 mm	235	8_10	1438	1438
322	SAC305	SAC105	1.0 mm	235	8_10	1800	1799
424	SAC305	SAC105	1.0 mm	235	8_11	1053	1053
426	SAC305	SAC105	1.0 mm	235	8_11	1308	1308
430	SAC305	SAC105	1.0 mm	235	8_11	1481	1481
520	SAC305	SAC105	1.0 mm	235	8_12	1873	1873
522	SAC305	SAC105	1.0 mm	235	8_12	1588	1589
526	SAC305	SAC105	1.0 mm	235	8_12	1538	1536

616	SAC305	SAC105	1.0 mm	235	8_13	1824	1824
618	SAC305	SAC105	1.0 mm	235	8_13	1600	1600
622	SAC305	SAC105	1.0 mm	235	8_13	1239	1238
690	SAC305	SAC105	1.0 mm	235	8_14	1652	1650
694	SAC305	SAC105	1.0 mm	235	8_14	1472	1472
76	SAC305	SAC105	1.0 mm	235	8_8	1722	1722
78	SAC305	SAC105	1.0 mm	235	8_8	1728	1728
82	SAC305	SAC105	1.0 mm	235	8_8	1753	1752
196	SAC305	SAC105	1.0 mm	235	8_9	1674	1674
198	SAC305	SAC105	1.0 mm	235	8_9	1742	1742
202	SAC305	SAC105	1.0 mm	235	8_9	1400	1400
14	SnPb	SAC 305	0.5 mm	215	2_1	2709	2724
19	SnPb	SAC 305	0.5 mm	215	2_1	6526	6526
23	SnPb	SAC 305	0.5 mm	215	2_1	3265	3265
134	SnPb	SAC 305	0.5 mm	215	2_2	2815	2815
139	SnPb	SAC 305	0.5 mm	215	2_2	2922	2923
143	SnPb	SAC 305	0.5 mm	215	2_2	2186	2186
254	SnPb	SAC 305	0.5 mm	215	2_3	2583	2582
259	SnPb	SAC 305	0.5 mm	215	2_3	3024	3026
263	SnPb	SAC 305	0.5 mm	215	2_3	2658	2659
374	SnPb	SAC 305	0.5 mm	215	2_4	2590	2591
379	SnPb	SAC 305	0.5 mm	215	2_4	2752	2752
383	SnPb	SAC 305	0.5 mm	215	2_4	2406	2407
470	SnPb	SAC 305	0.5 mm	215	2_5	2595	2597
475	SnPb	SAC 305	0.5 mm	215	2_5	3494	3494
479	SnPb	SAC 305	0.5 mm	215	2_5	2726	2726
566	SnPb	SAC 305	0.5 mm	215	2_6	2715	2715
571	SnPb	SAC 305	0.5 mm	215	2_6	2862	2862
575	SnPb	SAC 305	0.5 mm	215	2_6	2216	2216
659	SnPb	SAC 305	0.5 mm	215	2_7	2127	2127
663	SnPb	SAC 305	0.5 mm	215	2_7	2105	2105
62	SAC 305	SAC 305	0.5 mm	235	7_1	3467	3466
67	SAC 305	SAC 305	0.5 mm	235	7_1	3648	3648
71	SAC 305	SAC 305	0.5 mm	235	7_1	3916	3916

182	SAC 305	SAC 305	0.5 mm	235	7_2	2501	2501
187	SAC 305	SAC 305	0.5 mm	235	7_2	4435	4435
191	SAC 305	SAC 305	0.5 mm	235	7_2	2901	2901
302	SAC 305	SAC 305	0.5 mm	235	7_3	3795	3795
307	SAC 305	SAC 305	0.5 mm	235	7_3	3843	3843
311	SAC 305	SAC 305	0.5 mm	235	7_3	2891	2892
410	SAC 305	SAC 305	0.5 mm	235	7_4	3196	3196
415	SAC 305	SAC 305	0.5 mm	235	7_4	3442	3442
419	SAC 305	SAC 305	0.5 mm	235	7_4	3697	3698
506	SAC 305	SAC 305	0.5 mm	235	7_5	3542	3541
511	SAC 305	SAC 305	0.5 mm	235	7_5	3513	3513
515	SAC 305	SAC 305	0.5 mm	235	7_5	3235	3236
602	SAC 305	SAC 305	0.5 mm	235	7_6	3543	3543
607	SAC 305	SAC 305	0.5 mm	235	7_6	3648	3655
611	SAC 305	SAC 305	0.5 mm	235	7_6	3766	3765
683	SAC 305	SAC 305	0.5 mm	235	7_7	3560	3560
687	SAC 305	SAC 305	0.5 mm	235	7_7	3447	3447